THE CHANGE DETECTION OF BUILDING MODELS USING EPOCHS OF TERRESTRIAL POINT CLOUDS

Zhizhong Kang *, Zhao Lu

School of Land Science and Technology, China University of Geosciences, Beijing 100083, China - zzkang@cugb.edu.cn, edward_1986623@163.com

Commission VIII

KEY WORDS: Terrestrial laser scanning, Point cloud, Change detection, Emergency response, Hausdorff distance

ABSTRACT:

The highly detailed building modeling through terrestrial laser scanning has been studied in recent years. Among the applications of highly detailed models, change detection from street level, which has small scale, is relatively new and has good potential. Hence based on the rebuilt building models, we propose an approach of change detection of building models deploying different epochs of TLS data, which follows three steps: automatic point cloud registration, building model change detection and quantification of changed regions. The presented method only focuses on the disappearing change (for instance erosion, damage, etc.) of rebuilt building models and quantification of the changed regions, which can be helpful to the works, e.g. disaster management, insurance claim evaluation and so forth. Since the accuracy of terrestrial laser scanning is normally in the order of millimeter, the accuracy of the computed planar surface area is expected to reach the order of centimeter taking the error accumulation effect into consideration, which certainly can meet the need of the practical applications.

1. INTRODUCTION

The 5/12 Sichuan earthquake, Taiwan 8/8 floods, The 9/11 terrorist attacks, as well as other natural disasters are bitterly alarming us that complex 3D environments, at the street level, of urban built-up and highly populated areas considerably reduce the speed of emergency response, which consequently endangers civilians' lives and properties. Therefore, based on high resolution 3D digital models of densely populated areas, the extent of damage and impact areas can be determined, if changes in 3D models are able to be automatically detected after the disaster, which is of great importance for providing timely and reliable decision making of emergency response.

To date, detecting changes is mainly performed via images, usually by using object to background separation or a simple subtraction between images. Such models are limited and usually impose rigid constraints like static mounting of the camera, recognizable (usually artificial) landmarks, and are sensitive to shadows and local illumination problems.

TLS point cloud provided by high-resolution laser scanners is both dense and accurate, thereby allowing good applications of monitoring of changes that occur over time, for instance the need to update geographic information by comparing the existing information with current state, the close-ranged monitoring of the health conditions of transportation infrastructures and large-scale buildings during running or following disastrous events where comparison of pre- and post-events is required, etc. Although much attention has been paid to large-scale change detection (e.g. Murakami et al., 1999; Walter, V., 2004; Vogtle and Steinle, 2004; Matikainen et al., 2004), behavior of small size natural phenomena or changes of specific objects are of great importance for analyzing deformations or objects evolution, and require a more subtle

analysis of the measured scene. Concerning the change detection via terrestrial laser scans, several relevant researches have been proposed in recent years. The deformation analysis for designated objects has been discussed (Schäfer et al. 2004; Lindenbergh and Pfeifer, 2005; Gosliga et al., 2006). Girardeau-Montaut et al. (2005) carried out comparison by using the Hausdorff distance as a measure for changes. They pointed out three issues to be addressed, i.e. point sampling variations between scans, computation cost of the Hausdorff distance and real change discrimination. Zeibak and Filin (2007) also analyzed the potential artifacts that may affect the detection, which includes resolution and object pose variation, occlusion and scanner related artifacts (e.g. regions of no-reflectance, ranging limits, noise, etc.). They proposed an approach for change detection via TLS data that implement the comparison through a mere image subtraction between the range images of reference scan and analyzed scan transformed into the reference frame aiming to eliminate those artifacts. As this method considers the transformation parameters as known, the reliability of image subtraction depends greatly on the registration accuracy between reference and analyzed scans.

We propose in this paper an efficient algorithm for building model change detection based on a series of point cloud epochs over time and the rebuilt building models, which follows three steps: automatic point cloud registration, building model change detection and quantification of changed regions.

2. AUTOMATIC POINT CLOUD REGISTRATION

Because of the locations of scanning stations is not fixed, the coordinates of the same point in two adjacent scan epochs are not expected to be equal, so registration of the two epoch data is

---

* Corresponding author. *E-mail address*: zzkang@cugb.edu.cn..

required before the building change detection. Instead of the iterative closest point (ICP) and primitive-based methods, we adopt the approach to the automatic registration of terrestrial laser scanning (TLS) point clouds using panoramic reflectance images proposed by Kang et al. (2009). This method maps a 3D point cloud into a 2D reflectance image (Fig.1), which greatly simplifies the registration. The scale invariant feature transform (SIFT) method is utilized to make correspondence tracking feasible in the case of a panoramic stereo pair. Using the corresponding points detected in the previous step, transformation parameters between different coordinate frames are computed and thus the two point clouds are registered. In addition, the image point correspondence and our computation of the RTPs are integrated into an iterative process that allows for registration optimisation. Fig.2 illustrates the flowchart of the registration strategy.
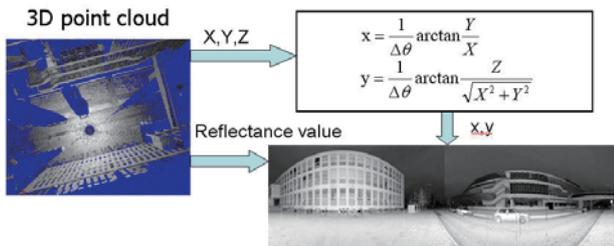
Figure 1 Procedure to construct the reflectance image from a 3D point cloud
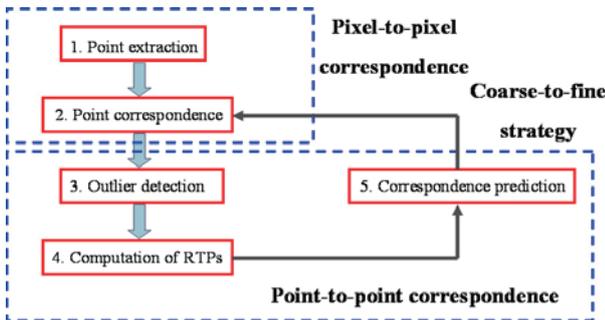
Figure 2 Flowchart of the registration strategy.

3. BUILDING MODEL CHANGE DETECTION

The forms of change mainly can be classified into deforming, disappearing, emerging and so on. Relevant researches has been reported on deforming (e.g. Schäfer et al. 2004; Lindenbergh and Pfeifer, 2005; Gosliga et al., 2006) and emerging (e.g. Girardeau-Montaut et al., 2005; Zeibak and Filin, 2007). As the related applications of highly detailed building models are discussed, we only focus on the disappearing change (for instance erosion, damage, etc.) of rebuilt building models and quantification of the changed regions, which can be helpful to the works, e.g. disaster management, insurance claim evaluation and so on. Therefore, the changed points are marked in the old scan instead of the new one.

The Hausdorff distance, or Hausdorff metric, measures how far two compact non-empty subsets of a metric space are from each other. In computer vision, the Hausdorff distance is used to find a given template in an arbitrary target image. Girardeau-Montaut et al. (2005) implemented point-to-point comparison by using the Hausdorff distance as a measure for changes and

an octree as a data structure for accessing the 3D point cloud. Inspired by this idea, an algorithm of change detection using TLS data is proposed in this section.

As Girardeau-Montaut et al. (2005) mentioned, the computation cost of the Hausdorff distance is a challenge to be faced. The change detection is carried out based on not only a series of point cloud epochs over time, but also the rebuilt building models (Fig.3). In this context, we only implement the comparison using the Hausdorff distance for the point segments both of the reference scan and analyzed scan transformed into the reference frame on each facet of the rebuilt building models. The computation time can be largely shortened as the searching range being narrowed remarkably by using this precondition. Since size is defined here in angular terms, the varying distance between consecutive points and scan-lines becomes inconsiderable. Moreover, the scanner related artifacts (e.g. regions of no-reflectance, ranging limits, noise, etc.) discussed by Zeibak and Filin (2007) cease being issues to be addressed as they should be eliminated from the old scan during the preceding modeling process.

Figure 3 the rebuilt building model
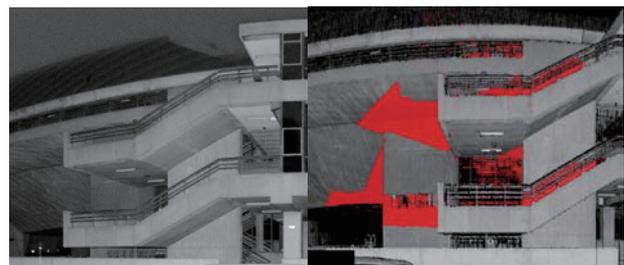
(a) The occluding scan   (b) The occluded parts highlighted in red

Figure 4 The occlusion due to scanning position change

At different epochs, occlusion of objects or object parts may occur as the scanning position changes. Fig.4 shows a scene part in 3D space (highlighted in red), which is seen in the right scan (a) but is occluded in the left one (b) due to the stairs. Those points appearing in one scan but not in the other are natural change candidates, which may lead to a likely consequence of false detection. To handle occlusion effects, Girardeau-Montaut et al. (2005) utilized the depth image generated from the scan, which is equivalent to a Z-buffer. As

Fig.1, the reflectance image used in the registration stage is similar to the depth image and thus it easily can be converted to the depth image by just replacing reflectance value with range. As for the detection of disappearing change, we transform the points marked as changed in the old scan into the local frame of the new one and compute their 2D coordinates in the depth image using Eq.1. The range values are compared between overlaying pixels. As a result, the transformed points with larger range values highlighted in red (Fig.4(b)) are considered as unchanged since they are occluded.

$$
\left.
\begin{aligned}
x &= \frac{1}{\Delta\theta}\arctan\frac{Y}{X} \\
y &= \frac{1}{\Delta\theta}\arctan\left(\frac{Z}{\sqrt{X^2+Y^2}}\right)
\end{aligned}
\right\} \quad (1)
$$

where x, y are the image coordinates of a point, whose ranges are determined by the FOV and angular resolution of the scan, X,Y, Z are the 3D coordinates, and $\Delta\theta$ is theangular resolution of the scan.

4. QUANTIFICATION OF CHANGED REGIONS

Since the result of changing detection using Hausdorff distance are a number of scattered points (Fig.5(a)), one need to quantify the changed regions before the applications of disaster management, insurance claim evaluation, etc. The volume of the changed region is certainly an optimal criteria of quantification if the accurate 3D model is known. However, the building models rebuilt using the method proposed by Pu and Vosselman (2009) made assumptions on the occluded and incompletely scanned areas to generate a solid polyhedron model, which leads to a geometric approximation of the whole building model. Therefore, instead of volume, we choose the planar surface area of changed regions on the building facade as the criteria of quantification in this context.

(a) The detected point segment
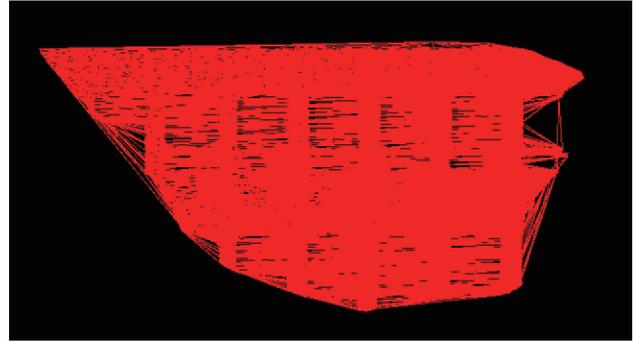
(b) The generated TIN

(c) The remained TIN mesh after excluding the holes and pointlessly triangles

Figure 5 The quantification of the changed region

To compute the planar surface area, we firstly generate a TIN (Triangulated Irregular Network) for the point segment marked as changed (Fig.5 (b)) on each facet of the rebuilt building models. As Fig.5 (b), the long TIN edges appear only at the outer boundary (wall outline) or inner boundary (holes) of a wall. Therefore, the triangles whose edges are longer than a certain threshold determined in terms of the sampling interval of the scan are removed from the generated TIN for the purpose of excluding the holes and pointlessly triangles made along the outer boundary from surface area calculation. Fig.5(c) shows that the remained TIN mesh accurately describes the distribution of the point segment in Fig.5(a) and then the planar surface area is computed using Eq.2 which is derived from Heron's Formula (Weisstein, 2010). If the changed region distributes on more than one planar facet, the planar surface area of the changed region is calculated through summing up Δ_{TIN} of each facet.

$$
\Delta_{TIN} = \sum_{i=1}^{n} \sqrt{s_i(s_i - a_i)(s_i - b_i)(s_i - c_i)} \qquad (2)
$$

where Δ_{TIN} = the area of the TIN mesh

n = the number of triangles of the TIN mesh

a_i, b_i, c_i = the lengths of the sides of triangle i

s_i = the semiperimeter of triangle i

s_i is computed as follow.

$$s_i = \frac{1}{2}(a_i + b_i + c_i) \qquad (3)$$

The accurately computed surface areas can be employed as a convincing ground to estimate the damage or erosion of the building facade, or evaluate the insurance claim.

5. EXPERIMENTAL RESULTS

A central area of the Dutch town Vlaardingen was scanned with a Leica terrestrial laser scanner in 6 scans. Different scans were coregistered and then geo-referenced to 2D map. The average point density is 500 points per square meter. Pu and Vosselman (2009) reconstructed the building facade models from the complete Vlaardingen dataset (Fig.6). Reconstructions of walls, doors and roofs are fully automatic, while some window edges are manually adjusted because many window decorations block a window part, especially the ones on the ground floor.
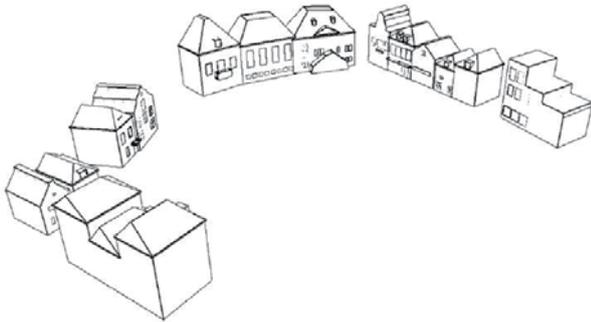
Figure 6 The reconstructed building facade models from the complete Vlaardingen dataset (Pu and Vosselman, 2009)

We picked out the building facade model illustrated as Fig.3 for change detection experiment. Fig.7 shows the point segment of one of rebuilt facades. We removed the blue part from the point segment supposing that it disappears due to damage. The comparison was implemented between the point segments before and after the removal. We assigned a random error within 1 centimeter to the coordinates of each point in the point segment after removal for simulating the registration error. As we mentioned in the preceding section, the comparison using the Hausdorff distance was only implemented for the point segments on the wall and roof of the rebuilt building model (Fig.8).
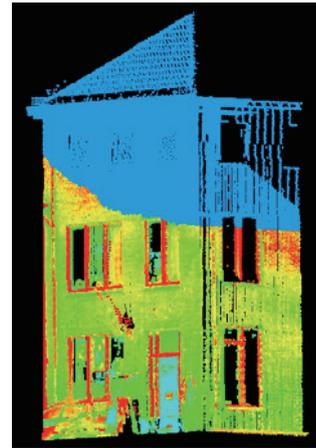
Figure 7 The point segment picked out
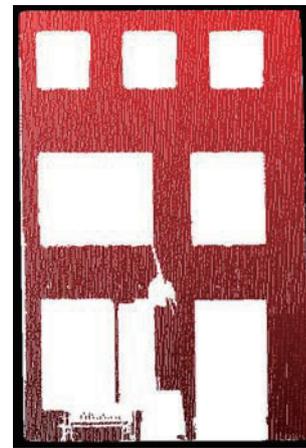
(a) The point segment on the wall
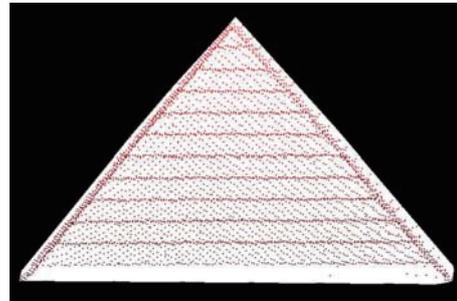
(b) The point segment on the roof

Figure 8 The point segments on the building facets

After the comparison, the detected region of change on the front wall is as Fig.9 (a). Following the steps of planar surface area computation proposed in section 4, a TIN mesh was generated from the point segment marked as changed. The triangles with long edges were eliminated from the generated TIN. Fig.9 (b) shows that the remained TIN mesh accurately describes the distribution of the point segment in general. The planar surface area was computed using Eq.2. Table 1 shows the change detection results in terms of the planar surface areas and the changed rate calculated via comparing them with those of the facets (e.g. wall, roof) before change. The planar surface area of

all of the changed regions on the roof, front wall and side wall was calculated through summing up Δ_{TIN} of each facet.
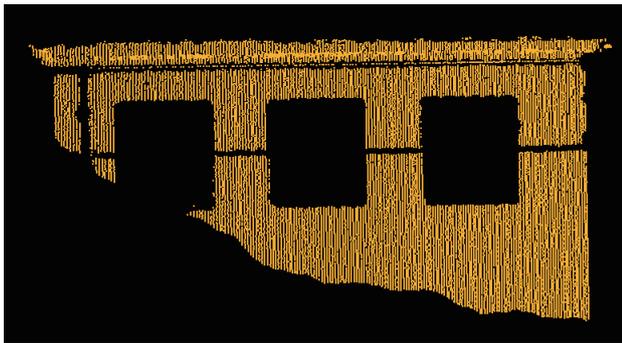
(a) The changed point segment
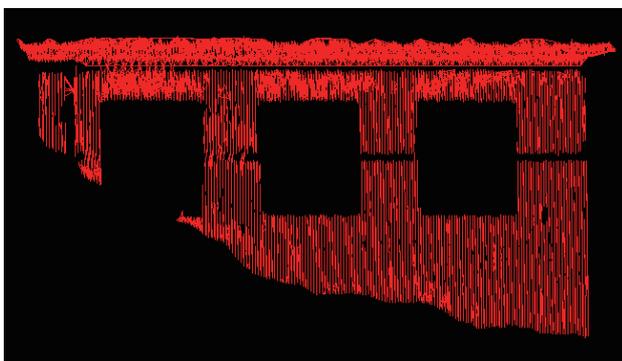
(b) The refined TIN mesh

Figure 9 The quantification of the changed region on the wall

Facet	Changed area (m²)	Facet area (m²)	Changed rate (percent)
Roof	12.22	12.22	100
Front wall	7.75	30.45	25.4
Side wall	11.35	35.79	31.7
Total	31.32	78.46	39.9

Table 1 The change detection results

Since the accuracy of terrestrial laser scanning is normally in the order of millimeter, the accuracy of the computed planar surface area is expected to reach the order of centimeter taking the error accumulation effect into consideration, which certainly can meet the need of the applications of disaster management, insurance claim evaluation, etc.

6. CONCLUSIONS

The experiment has been implemented on the TLS data. The result of change detection shows that the Hausdorff distance is a good solution for change detection. It also reveals that the changed regions can be accurately described through constructing a TIN from the scattered points and excluding the holes and pointlessly triangles made along the outer boundary. The succedent quantification of the changed regions which is of great importance to the applications of disaster management,

insurance claim evaluation and so on, is believed to reach the centimeter-order accuracy.

Future work will concentrate on the optimization of Hausdorff distance detection algorithm in terms of the computation cost, registration accuracy, etc.

REFERENCE

Girardeau-Montaut, D., Roux, M., Marc, R., Thibault, G., 2005. Change detection on points cloud data acquired with a ground laser scanner. International Archives of Photogrammetry, Remote Sensing. 36(3/W19), 30-35

Gosliga van R., Lindenbergh, R., Pfeifer, N., 2006. Deformation Analysis of a Bored Tunnel by Means of Terrestrial Laser scanning. Image Engineering and Vision Metrology, ISPRS Symposium, Dresden.

Kang, Z., Li, J., Zhang, L., Zlatanova, S., 2009. Automatic Registration of Terrestrial Point Clouds using Reflectance Panoramic Images, Sensors, 9, doi: 10.3390/sensors.

Lindenbergh, R., Pfeifer, N., 2005. A statistical deformation analysis of two epochs of terrestrial laser data of a Lock. In: Proceedings of the 7th Conference on Optical 3-D measurement techniques, Vienna.

Matikainen, L., Hyyppä, J., Kaartinen, H., 2004. Automatic detection of changes from laser scanner and aerial image data for updating building maps. In: The International Archives of the Photogrammetry, Remote Sensing and Spatial Information Sciences, Istanbul, Turkey, 35(B2), 434-439.

Murakami, H., Nakagawa, K., Hasegawa, H., Shibata, I., Iwanami, E., 1999. Change detection of buildings using an airborne laser scanner. ISPRS Journal of Photogrammetry and Remote Sensing, 54(2-3), 148-152.

Pu, S., Vosselman, G., 2009. Knowledge based reconstruction of building models from terrestrial laser scanning data, ISPRS Journal of Photogrammetry and Remote Sensing, 64(6), 575-584.

Schäfer, T., T. W., Kyrinovič, P., Zámečniková, M., 2004. Deformation Measurement Using Terrestrial Laser Scanning at the Hydropower Station of Gabčíkovo, In: Proceedings of INGEO 2004 and FIG Regional Central and Eastern European Conference on Engineering Surveying. Bratislava, Slovakia.

Vogtle, T., Steinle, E., 2004. Detection and recognition of changes in buildings geometry derived from multitemporal laserscanning data. International Archives of Photogrammetry and Remote Sensing, 35(B3).

Walter, V., 2004. Object-based classification of remote sensing data for change detection, ISPRS Journal of Photogrammetry and Remote Sensing, 58(3-4), 225-238.

Weisstein, Eric W., 2010. "Heron's Formula." From MathWorld--A Wolfram Web Resource. http://mathworld.wolfram.com/HeronsFormula.html.

Zeibak, R. and Filin, S., 2007. Change detection via terrestrial laser scanning. IASPRS, 36(3), 430–435.